International Journal of Geography and Geography Education (IGGE)

To Cite This Article: Karabulut, M. & Küçükönder, M. (2019). An examination of temporal changes in Göksu Delta (Turkey) using principle component analysis. *International Journal of Geography and Geography Education*, 39, 279-299.

Submitted: August 28, 2018 **Revised:** September 29, 2018 **Accepted:** October 13, 2018

AN EXAMINATION OF TEMPORAL CHANGES IN GÖKSU DELTA (TURKEY) USING PRINCIPLE COMPONENT ANALYSIS

Anabileşen Tekniği Kullanılarak Göksu Deltasında (Türkiye) Zamansal Değişikliklerin İncelenmesi

Murat KARABULUT[1]

Muhterem KÜÇÜKÖNDER[2]

Öz

Kıyı alanları, ekolojik ve ekonomik değeri yüksek doğal ortamlar arasında yer alır. Diğer doğal sistemler arasında, özellikle deltalar dinamik ve karmaşık ilişkilere sahip ekosistemlerdir. Bu çalışma, Türkiye'nin Akdeniz bölgesinde bulunan Göksu Deltası'nı kapsamaktadır. Göksu Deltası birçok nesli tükenme tehlikesi altında olan türe, üreme, beslenme ve barınma olanakları sunan, en önemli uluslararası sulak alanlarından birine sahiptir. Göksu Deltası'nda hidrolojik müdahaleler ve çeşitli insan faaliyetleri sonucunda delta kıyı sistemleri büyük ölçüde değişmiştir. Bu değişimlerin efektif bir şekilde incelenmesi zorunludur. Bu amaca yönelik olarak çeşitli uydu sistemlerinden elde edilen uzaktan algılanan verilerin, dijital veya analog teknikleri kullanarak kıyı değişikliklerini izlemek için etkili bir araç olduğu kanıtlanmıştır. Böylelikle, son yıllarda, kıyı alanlarının çoğunun haritalanması ve izlenmesi, bu tür veriler tarafından sağlanan mekansal açıdan kapsamlı bilgilerle ortaya konmuştur. Çalışmanın amacı Göksu Deltası'ndaki kıyı değişikliklerini Ana Bileşenler Analiz tekniğini kullanarak incelemektir. Sonuçlar, bu yöntemin, multitemporal görüntüleri kullanarak değişim tespitindeki hataları azaltabileceğini ve değişikliklerini izlemede çok faydalı bir yol sağlayabileceğini göstermektedir. Kıyı ilerlemesi batı ve güneydoğuda tespit edilmiştir. Öte yandan, deltanın doğu tarafında sahil şeridinde ciddi bir gerileme meydana gelmiştir.

Anahtar Kelimeler: Kıyı Değişimi, Zamansal Değişim, Göksu Deltası, Uzaktan Algılama, PCA

Abstract

Coastal areas are natural systems with high ecological and economic value. Among other natural systems, deltas are the ecosystems with the most dynamic and complex relations. This study comprises of Göksu Delta which is located in the Mediterranean region of Turkey. Göksu Delta have one of the most important international wetlands that provide reproduction, nutrition and accommodation facilities for delicate, rare and in danger of extinction of many species. As a result of the hydrologic interventions and several human activities in Göksu Delta, coastal systems of Göksu Delta have been changed drastically. Remotely sensed data, which have obtained from several satellite systems, have proven to be an effective tool for monitoring coastal changes using digital or analog techniques. Thus, in recent years, most mapping and monitoring of coastal areas has been dependent on the use of remotely sensed data, because of the spatially comprehensive view provided by such data. The aim of this is to examine coastal changes in Göksu Delta using principle component analysis. The study demonstrates that this method can reduce errors in change detection using multitemporal images and provide a very useful way in monitoring rapid coastal changes. Coastal progression was detected in the west and southeast. On the other hand, there is a severe regression in the coastal line at the eastern side of the delta.

Keywords: Coastal Change, Temporal Change, Göksu Delta, Remote Sensing, PCA

[1] **Correspondence to:** Prof., Kahramanmaraş Sütçü İmam University, Faculty of Sciences and Arts, Department of Geography, Third floor, Room Number: 24, Avşar Campus, 46100, Kahramanmaraş, TURKEY., *https://orcid.org/0000-0002-1456-6908.*, mkarabulut@ksu.edu.tr

[2] Assist. Prof., Kahramanmaraş Sütçü İmam University, Faculty of Sciences and Arts, Department of Geography, Third floor, Room Number: 16, Avşar Campus, 46100, Kahramanmaraş, TURKEY., *https://orcid.org/0000-0001-5350-7794.*, mhtrm.kckndr@gmail.com

INTRODUCTION

Deltas where major rivers reach the sea are geographically unique, ecologically and socioeconomically significant landscape of the world and sustaining many species both plant and animal and provide home for several hundred million people. Deltas are important areas, locating transition zones between terrestrial and marine environments (Hinrichsen, 1998). Therefore, deltas contribute greatly to biomass production and acting an important role in the biochemical cycles (Mitsch and Gosselink, 2000; Özesmi and Bauer, 2002; Karabulut, 2007). Deltas provide several advantages for human activities due to smooth and plain topography, existing resources of fresh and salt water, easy transportation via Marine, land and river ways and suitability for agriculture. However, all these intense activities make deltas that are environments with high risk of several natural and human induced problems. Large and increasing extent of human activities in delta areas has enhanced or caused several kinds of environmental problems in the world and Turkey.

These valuable areas are experience quick and significant modifications in composition, character, structure and size driven by human related activities. These dramatic and continuous alterations keep the potential to widely affect ecologic and socio-ecologic functioning amongst delta systems. In delta areas quality and quantity of natural habitats have been damaged because of the reclamation of land for settlement related activities such as urban and industrial development, agriculture, and tourism. River deltas of Turkey especially are reflected to be under risk of extensive modification because of the human related activities. It is thus important that the quantification and characterization of types and conditions of deltas are required for sustainable use of such resources and for better understanding the impact of changes in those areas via technology based approaches (Özesmi and Bauer, 2002; Zhang et al., 2011).

Mapping and monitoring is crucial for the sustainable delta management. Land use/cover maps can be used to assessment and management of delta environments. Reliable delta land cover/use maps are required for monitoring temporal changes, for quantifying or assessing natural habitat conditions and examining their access to other ecosystem components which directly or indirectly related to them.

The data from remote sensing systems provide an effective toll against ground based data collection techniques and archive information about landscape scale condition (Özesmi and Bauer, 2002). Because of their continuous repetitive nature, remote sensing data are useful for monitoring changes in deltas such as dune progression and regression over longer time span. Moreover, the remotely sensed data can be recorded at more varies temporal and spatial scales than what is commonly accomplished with field studies (Adam et al., 2010). Traditional field based data collection methods are time consuming, expensive and labor intensive. Those traditional techniques can also provide only point data which are generally not enough to cover entire habitat. In contrast, remote sensing is an economical way to monitor wetland areas, because it can cover large areas in a short time on a repetitive basis.

Scientists and Resource managers are therefore interested in deltas using such data, because this method provides continuous data for desired extents. Several studies represented that examination of medium resolution satellite data (such as Landsat TM, SPOT) can successfully provide the ecologic conditions of deltas (Zhang et al., 2011; Ghioca-Robrect et al., 2008; Gilmore et al., 2008; Hardisky et al., 1986; Lunetta and Barlogh, 1999; Rundquist et al., 2001; Tsai et al., 2007; Silva et al., 2008; Adam et al., 2010; De Roeck et al., 2008; Mishra et al., 2006).

Nevertheless, over heterogeneous or non-uniform delta areas, remote sensing techniques are delimiting to only rely on common classification methods (supervised and unsupervised) to collect information about land use/cover changes (Ullah et al., 2000; Özesmi and Bauer, 2002; Artigas and Yang, 2006). The incorporation of PCA, which is based on data reduction procedures, potentially offers the ability to detect changes efficiently (Deng et al., 2008; Lu et al., 2004; Li and Yeh, 2010; Balázs et al., 2018).

In this study, historical process of natural and unnatural changes in Göksu Delta will be examined by using PCA. Magnitude and locations of these changes can be analyzed. Our results will be important in the development of appropriate remote sensing techniques for mapping and monitoring delta habitat health and functioning.

MATERIAL AND METHOD

The present study was carried out in the Göksu delta which is located in the Mediterranean region of Turkey (Figure1x). The climate of the area is typically Mediterranean characterizing with hot and dry summer, cool and rainy winter (Karabulut, 2015). The Delta have one of the most important international wetlands that provide reproduction, nutrition and accommodation facilities for delicate, rare and in danger of extinction of many species and 43 which are rarely found species across the country are under threat (Gürkan et al., 1999; Yıldırım et al., 2009). This area is also located on the one of the world's important bird migration route. In Turkey, approximately 450 bird species have been identified and 332 of them have been observed in the Göksu Delta. Globally, 12 endangered bird species out of 24 were also found in the Göksu Delta. Flora of the area consists of 384 taxa and among these, 5 of them on a global scale, 3 of them on the European scale are under risk due to human population growth and economic development. Göksu Delta is subjected to a multiple resource use conflict, overexploitation of coastal resources and environmental degradation (Gürkan et al., 1999; Yıldırım et al., 2009). This has resulted in a change to the coastal landscape and a reduction and fragmentation of habitat. In order to better protect coastal wetland ecosystem and biodiversity in the study area, periodic mapping of land use and coastal habitats should be performed to observe trends and changes. In this study, a multi-temporal and multispectral image data set was used to determine changes of land cover/use and coastal area in Göksu delta, Turkey.

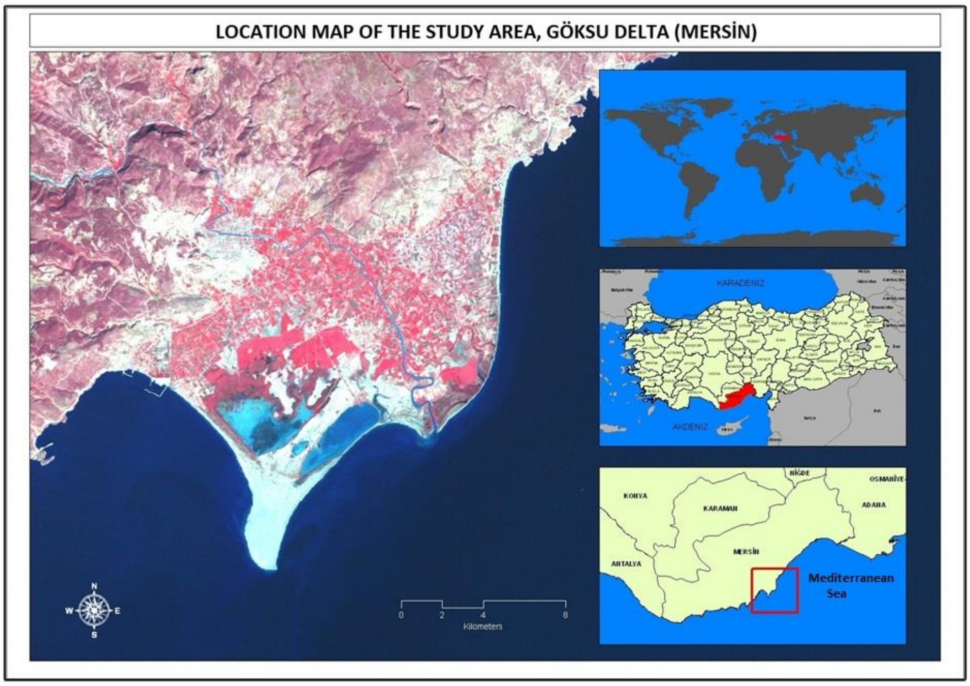

Figure 1: Location Map of the Study Area

In the first stage the images were subject to radiometric and geometric pre-processing before transformation of PCA, as explained below.

Image Data

The selection of remote sensing images from different years is an important step in change detection analysis due to their direct impact on the results. In addition, Image properties (cloudiness, fog and haze) as well as the general characteristics of the study area are also important. A combination of Landsat Thematic Mapper (TM) and ETM images was used due to availability. The satellite images were from July and August 1984, 1990, 2000, 2010 and 2011 (Table 1). The satellite images were from July and August 1984, 1990, 2000, 2010 and 2011 (Table 1). TM has 7 and ETM has 8 spectral bands, including a panchromatic and thermal bands: Band 1 Visible (0.45 - 0.52 µm) 30 m, Band 2 Visible (0.52 - 0.60 µm) 30 m, Band 3 Visible (0.63 - 0.69 µm) 30 m, Band 4 Near-Infrared (0.77 - 0.90 µm) 30 m, Band 5 Near-Infrared (1.55 - 1.75 µm) 30 m, Band 6 Thermal (10.40 - 12.50 µm) 60 m. An effort was made to acquire images as close as possible to anniversary dates. In order to reduce spectral confusion that occurs between wetland plants and other vegetation types in the interpretation and analysis of images, summer images which represent wetland plants in different height and density are preferred. This procedure, at the same time, prevents errors that occur in seasonal variation of images. Images from months of July and August (dry months in the area) were selected based on cloudiness.

Pre-Processing Phase

The 2011 image was geometrically corrected and geo-referenced to the Universal Transverse Mercator (UTM) projection using the nearest neighbor resampling algorithm. Using this rectified image as the baseline, the other images were registered to it. Image co-registration process minimizes the offset between multi-date images of the same area, which can be generally quite noticeable, if such images were rectified individually.

In order to find out differences and similarities in spectral reflectance values of the raw images, radiometric statistics are calculated for all images (Table 1). It was evaluated visually by comparison with corresponding wavelength combinations in the statistics. 4, 3 and 2 (Red, Green, Blue: RGB) band combinations were examined visually for all five years of Landsat satellite images.

Table 1: General Statistics of Landsat Images

Basic Statistics		Min.	Max.	Mean	S. Dev.
03 August 1984	1 (Blue)	68	255	98.47	18.94
	2 (Green)	22	140	39.29	15.67
	3 (Red)	9	178	35.15	22.88
	4 (NIR)	1	190	44.28	39.17
	5 (MIR)	1	255	49.69	54.84
	7 (MIR)	1	248	26.21	29.43
04 August 1990	1 (Blue)	75	241	101.85	14.83
	2 (Green)	24	128	41.03	13.98
	3 (Red)	18	159	36.69	21.27
	4 (NIR)	9	157	39.93	33.25
	5 (MIR)	4	255	50.08	52.50
	7(MIR)	3	153	26.97	28.59
30 July 2000	1 (Blue)	80	184	101.88	12.02
	2 (Green)	19	173	43.29	12.31
	3 (Red)	23	154	43.40	20.82
	4 (NIR)	15	145	42.13	29.87
	5 (MIR)	11	250	54.62	50.80
	7 (MIR)	6	143	29.66	27.50
27 August 2010	1 (Blue)	56	226	84.02	15.54
	2 (Green)	16	143	35.52	13.99
	3 (Red)	11	203	33.61	21.85
	4 (NIR)	5	185	37.33	32.22
	5 (MIR)	1	255	48.11	50.25
	7 (MIR)	2	183	25.26	26.31
13 July 2011	1 (Blue)	81	201	106.41	12.28
	2 (Green)	30	126	47.41	12.13
	3 (Red)	25	178	47.91	19.37
	4 (NIR)	16	172	46.16	28.02
	5 (MIR)	13	255	62.90	49.16
	7 (MIR)	8	255	33.72	25.49

It is observed that the activity cycle of plants where agricultural activities common such as paddy fields in July images of 2000 and 2011 displays differences in other years (Figure 2). This causes to increase mean of the TM4, TM2 and TM3 bands for the years of 2000 and 2011 as compared to other dates. Likewise standard deviation of TM4 band is calculated to be low due to a more homogenous distribution of the data. Spectral reflectance values in these wavelengths for wetland plants represent no significant visual difference with other type vegetation reflections. Moreover, bare lands and dune areas in this band combination provide similar reflection for each wave length. In general, the prevailing water surface is lowered average reflectance values at each wavelength in the study area.

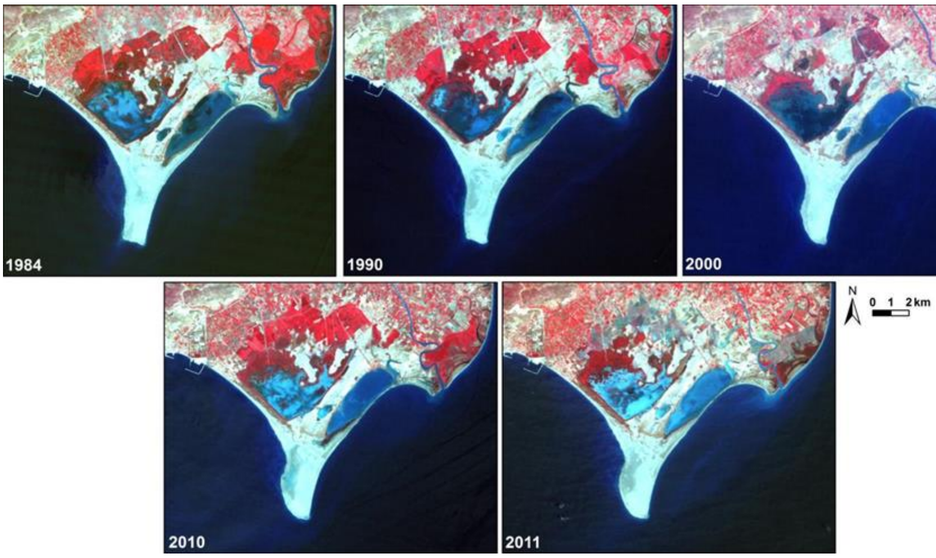

Figure 2: Landsat TM images (RGB: 432) used in PCA

Band 1 for images from all the years (Blue 0,45-0,52 µm) shows the highest average and the lowest standard deviation values. This result comes from concentration of the reflections from the water surfaces in the TM1 band wavelength range and insignificant impact of land and vegetation reflections on the image statistics for the study area. In contrast, TM4 and TM5 bands indicate higher standard deviation and lower mean values due to the reflection characteristics of vegetation and sand dunes (Figure 3).

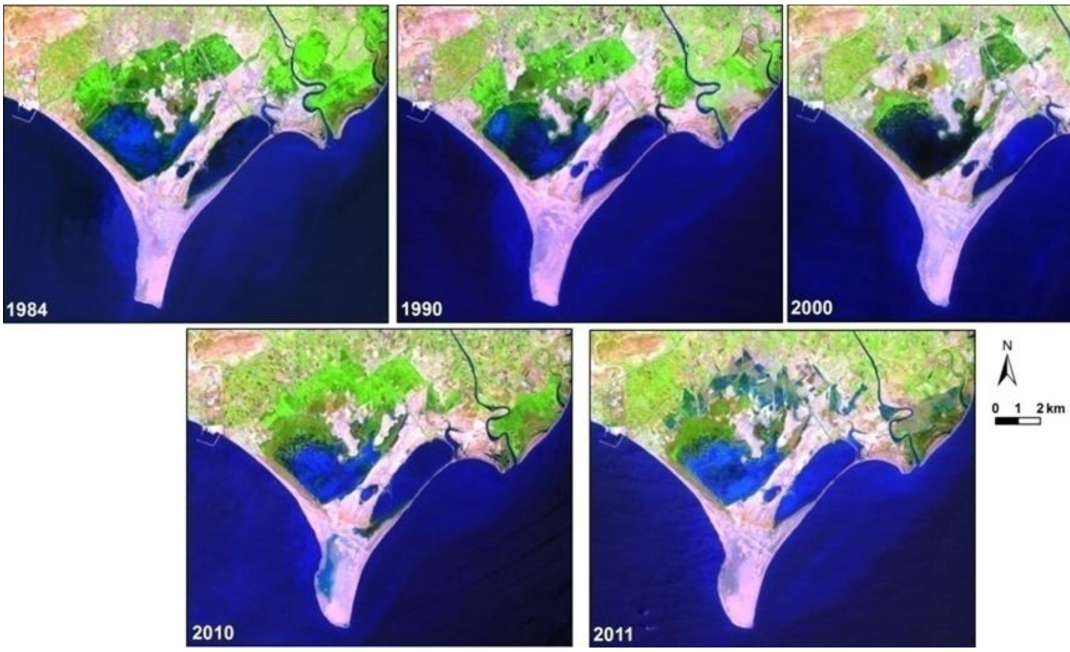

Figure 3: Combination of Landsat TM5, TM4 and TM1 bands (RGB: 541)

The highest standard deviation (average fifty for all years) and the second highest mean values are calculated for Band 5 (1, 55 to 1,75 µm). At this wavelength, in addition to reflections from the uncovered areas, especially reflection values of vegetation on the dune fields become more obvious. This result indicates that TM 5 and TM 4 bands have high variance due to the diversification of the image content. Plants cycles in agricultural areas are distinguished in different shades of green on the TM 5, TM4 and TM1 combination image. This tonal difference can be associated with high reflection of vegetated surfaces in the infrared band.

Burnt land is separated clearly from surrounding wetland plants on the image of 2000 (TM 5, TM4 and TM1 band combination) due to the low saturation rate of TM1. Based on these results, it can be said that TM5 is useful during the distinction of vegetation and soil properties. Reflections represent variation in agricultural areas for all years due to the changing nature of agricultural practices and differences in image acquisition months. These differences are taken into account when evaluating the results of the change analysis.

It is seen that there is generally high inter-band correlation for all images (Table 2). Bands of blue, green and red (TM1, TM2 and TM3) which are in the visible region of the electromagnetic spectrum and mid-infrared bands of TM5 and TM7 indicate high inter-band correlations. According to the correlation results, the lowest correlations were gained for TM1 and TM4 bands which mean that the bands contain different information. Although there is a clear distinction between the visible and infrared wavelengths, TM3 is highly correlated with the bands of TM5 and TM7 for all images that used in this study. This high inter-band correlation can be related to similar reflections from soil and sand dunes with low moisture content and also associated with a strong absorption in the infrared region of the water surface (Figure 4). Dune areas where organic matter (dune vegetation litter) increased and wet surfaces have become more visible in the band combination of TM7, TM5 and TM3.

Table 2: Correlation Values Between Landsat TM Image Bands

	Correlations	TM 1	TM 2	TM 3	TM 4	TM 5	TM 7
03 August 1984	TM 1	1,000000					
	TM 2	0,907191	1,000000				
	TM 3	0,855742	0,973579	1,000000			
	TM 4	0,411051	0,702782	0,747406	1,000000		
	TM 5	0,657864	0,844830	0,913308	0,880842	1,000000	
	TM 7	0,727940	0,871338	0,938008	0,812590	0,984728	1,000000
	Korelasyon	TM 1	TM 2	TM 3	TM 4	TM 5	TM 7
04 August 1990	TM 1	1,000000					
	TM 2	0,895565	1,000000				
	TM 3	0,850336	0,974563	1,000000			
	TM 4	0,432375	0,736397	0,768285	1,000000		
	TM 5	0,688769	0,878174	0,934457	0,889025	1,000000	
	TM 7	0,756075	0,899423	0,955644	0,818181	0,984023	1,000000
	Korelasyon	TM 1	TM 2	TM 3	TM 4	TM 5	TM 7
30 July 200	TM 1	1,000000					
	TM 2	0,897530	1,000000				
	TM 3	0,839792	0,973973	1,000000			
	TM 4	0,582795	0,832441	0,884013	1,000000		
	TM 5	0,711850	0,891747	0,948976	0,954336	1,000000	
	TM 7	0,765965	0,909206	0,962332	0,917018	0,987954	1,00
	Korelasyon	TM 1	TM 2	TM 3	TM 4	TM 5	TM 7
27 August 2010	TM 1	1,000000					
	TM 2	0,869703	1,000000				
	TM 3	0,783494	0,964087	1,000000			
	TM 4	0,318529	0,668182	0,753317	1,000000		
	TM 5	0,527751	0,792385	0,890993	0,907233	1,000000	
	TM 7	0,614276	0,826660	0,918506	0,834392	0,980856	1,000000
	Korelasyon	TM 1	TM 2	TM 3	TM 4	TM 5	TM 7
13 July 2011	TM 1	1,000000					
	TM 2	0,892007	1,000000				
	TM 3	0,790269	0,960255	1,000000			
	TM 4	0,371663	0,698585	0,802350	1,000000		
	TM 5	0,469096	0,734465	0,857596	0,933520	1,000000	
	TM 7	0,546200	0,762454	0,879159	0,874062	0,981063	1,000000

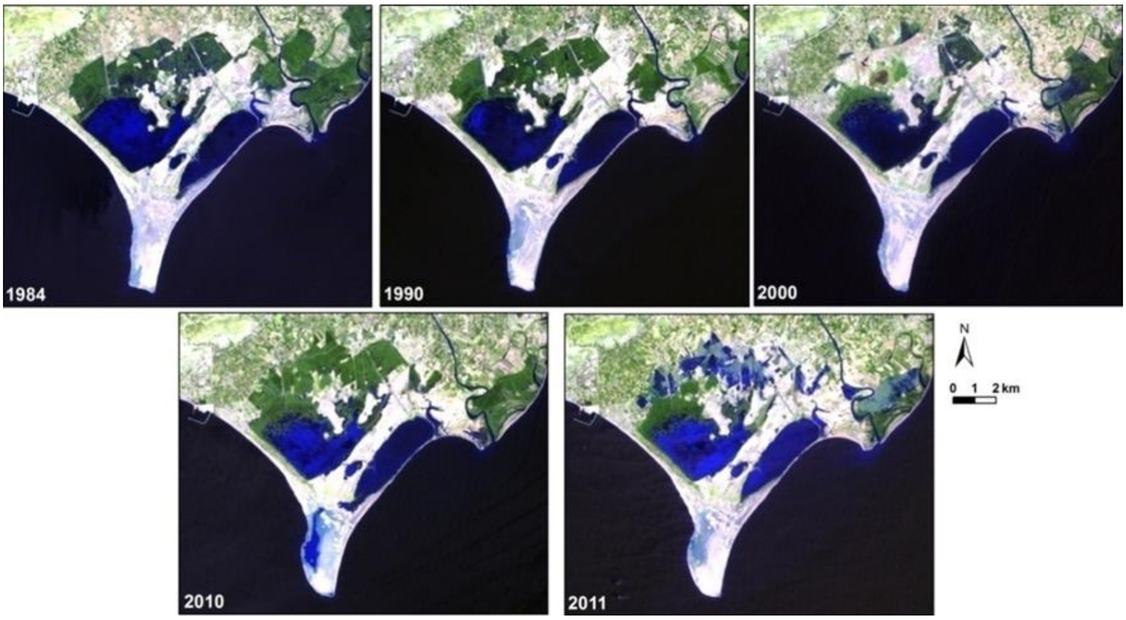

Figure 4: Landsat TM7, TM5 and TM3 Band Combination (RGB: 753) Which Separates Water Surfaces and Plant

PCA

Data sets that are obtained through the satellites can be analyzed in different ways in order to achieve information about land cover change through time. One of these methods is Principal Components Analysis (PCA). It is difficult to determine temporal changes when the correlation is high among the values of image data in bands for most of the time. The PCA method reduces the dimensionality of the data set through a mathematical transformation and less correlated new data set is obtained from the original band values (Jensen, 1996). In this method, although it is difficult to analyze the meaning of components of each image, the results are meaningful and can be used in the different change detection studies (Lu et al., 2004; Deng et al., 2008; Almutairi and Warner, 2010). Therefore, remote sensing data can be better interpreted due to dimensionality reduction of raw data by PCA. Theoretically, it is possible to visually observe the change in the image due to the changed pixel values showing low a correlation and unchanged values constituting high correlation.

Although PCA is not a new method, the use of the method for different purposes varies nowadays (Lu et al., 2004; Munyati, 2004; Ortiz-Rivera et al., 2006; Deng et al., 2008; Li and Yeh, 2010; Kassawmar et al., 2011; Balázs et al., 2018). Mathematically the procedure can be summarized in three stages. Firstly, Covariance or correlation matrices are generated for the data set and secondly, Eigen values and vectors are obtained. In the final phase, the main component values are calculated and new images are created from the final data set.

PCA is used in many studies in the monitoring of changes occurring in wetlands (Munyati, 2004; Ortiz-Rivera et al., 2006; Kassawmar et al., 2011). In order to determine changes in coastal and wetland areas in the Göksu Delta, the appropriate band combinations have been determined for PCA analysis by using different wavelength combinations. For this purpose, in the study, first of all the PCA technique was applied on all wavelengths of data sets from different years separately. Thus, we aimed to investigate the changes of the field. Secondly, TM2, TM3, TM4 and TM1, TM4, TM5 combinations are used during the transformation of the main components in the study area. TM2, TM3 and TM4 bands are decided as the appropriate combination based on preliminary results and these wavelengths are combined for all years. Images generated from PCA were evaluated for change detection analysis and appropriate PCs were classified by using unsupervised classification method to calculate change areas.

RESULTS AND DISCUSSIONS

General PCA

Correlation matrices were calculated in the first phase of the PCA by using images of all years used in this study. Eigen values and matrices were generated from the original (raw) data set and the component images were produced in the second step. First and second principle component images, as expected, contain approximately 95% of the full image data (Table 3). The first principal component for each data set containing six bands (PC1) has approximately 90% of the variance, while the sixth component (PC6) represents an average of only 0.04% on the entire data set.

Table 3: Eigenvalues and Vectors of Image Data Set

03 August 1984	Eigen Vectors	PC 1	PC 2	PC 3	PC 4	PC 5	PC 6
	TM 1	0,168890	0,179467	0,278118	0,463730	0,711196	0,375597
	TM 2	0,565767	0,255543	0,316541	-0,690401	0,025844	0,192574
	TM 3	-0,438817	-0,384967	-0,259704	-0,518304	0,480150	0,304320
	TM 4	0,634528	-0,232634	-0,717945	0,105145	0,128491	-0,015664
	TM 5	0,019231	-0,189845	-0,005522	0,156561	-0,496181	0,832377
	TM 7	-0,236279	0,814942	-0,489418	-0,063985	-0,016816	0,190091
	Eigen Values	5873,873	485,249	145,685	19,383	8,428	2,794
	%	89,88	7,42	2,23	0,29	0,13	0,043

04 August 1990	Eigen vectors	PC 1	PC 2	PC 3	PC 4	PC 5	PC 6
	TM 1	0,146714	0,176491	0,281909	0,421538	0,73212	0,392622
	TM 2	-0,507331	-0,228330	-0,309010	0,735150	-0,02294	-0,232433
	TM 3	0,463790	0,443841	0,296667	0,477343	-0,43339	-0,290188
	TM 4	-0,661792	0,201011	0,688923	-0,082690	-0,18037	0,087399
	TM 5	0,058003	-0,133660	-0,115480	0,196310	-0,49182	0,827655
	TM 7	0,254275	-0,813300	0,499077	0,092889	-0,03495	-0,122322
	Eigen values	5107,533	329,308	87,128	14,724	7,684	2,297
	%	92,05	5,93	1,57	0,27	0,14	0,041

30 July 2000	Eigen vectors	PC 1	PC 2	PC 3	PC 4	PC 5	PC 6
	TM 1	-0,128562	-0,163460	-0,291285	-0,416435	-0,736345	-0,395327
	TM 2	0,615867	0,321267	0,373013	-0,576445	-0,101834	0,188938
	TM 3	-0,253081	-0,393345	-0,289544	-0,632422	0,411624	0,357774
	TM 4	0,677752	-0,121664	-0,691996	0,165056	0,124284	-0,065589
	TM 5	0,017296	-0,156670	-0,065904	0,243120	-0,512271	0,805781
	TM 7	-0,283696	0,822193	-0,457139	-0,089355	0,011100	0,162578
	Eigen Values	4737,904	151,142	49,332	12,281	6,824	2,050
	%	95,53	3,047	0,99	0,24	0,13	0,041

27 August 2010	Eigen vectors	PC 1	PC 2	PC 3	PC 4	PC 5	PC 6
	TM 1	0,130493	0,171368	0,294300	0,433841	0,732370	0,377372
	TM 2	0,626280	0,341823	0,393363	-0,553229	-0,096332	0,144406
	TM 3	-0,274705	-0,341441	-0,231278	-0,660822	0,418805	0,377334
	TM 4	0,677470	-0,205227	-0,683340	0,144640	0,100607	0,030310
	TM 5	-0,016547	-0,157625	0,035413	0,211411	-0,518330	0,812567
	TM 7	-0,236731	0,818684	-0,486781	-0,058464	-0,012988	0,182132
	Eigen values	4661,163	365,618	110,952	22,416	8,139	3,228
	%	90,13	7,06	2,14	0,43	0,15	0,062

2011 July 13	Eigen Vectors	PC 1	PC 2	PC 3	PC 4	PC 5	PC 6
	TM 1	0,100979	0,148730	0,269769	0,410701	0,758898	0,387693
	TM 2	0,640589	0,444698	0,503702	-0,292197	-0,222536	0,057208
	TM 3	-0,010688	-0,214159	-0,172767	-0,795009	0,308235	0,443988
	TM 4	-0,678696	0,018423	0,708911	-0,171085	-0,082641	0,019430
	TM 5	-0,008971	-0,142518	-0,019173	0,282716	-0,521643	0,791960
	TM 7	-0,344421	0,844753	-0,375151	-0,068609	-0,024527	0,147372
	Eigen values	4155,614	249,618	98,419	12,692	7,964	1,974
	%	91,81	5,51	2,17	0,28	0,17	0,043

Topographic effect is more pronounced in the analysis of the principal components (PC1) because generally all reflections give positive load factor (Liu and Mason, 2009). Reflection properties in all major components starting from the first component are related to mostly land cover types for the study area. Topographic effect is undetectable due to the low altitude and insignificant slope changes in the Göksu delta. PCs are composed of positive and negative factor loads at different wavelength intervals in multi-temporal data sets (Yana and Ichikawa, 2007). This has resulted in different characteristics of image data sets due to changes in wetland ecosystem and other geographical features of the region as well as changes in 27 years.

PC1 (TM4 and TM2) provides a high positive load factor in the green and near-infrared wavelength region (0,566 and 0,634, respectively) and a high negative load factor in the red zone (-0,438) for the principle component image of 1984. In PC2 component, load factors are low in the visible wavelengths of red and green (0.255 and -0.385, respectively), on the other hand, the mid-infrared region (TM7) represented quite a high load factor (0.815). Near-infrared (TM4) produces negative high load factors (-0.718) in the PC3 component. On the 1984 image, PC1, PC2 and PC3 components highlight reflection characteristics of vegetation, dune areas and water surfaces (Figure 5). Maroon colored areas correspond to agriculture and yellows donate sand dunes in PC images of 1984, 2010 and 2011. Green and blue tones represent surface water according to changes in the content of the sediment concentration.

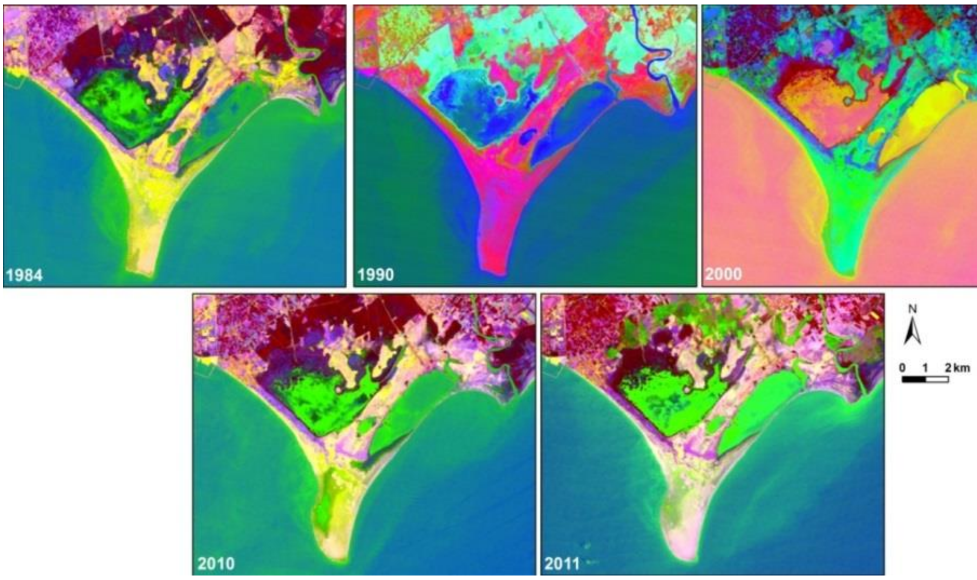

Figure 5: Landsat TM PCA Images (RGB: PC1, PC2, PC3)

The first principal component image of 1984 and 1990 has the high negative load for the bands of TM2 and TM4 (-0.507 and -0.662, respectively) and the highest positive load value is obtained as 0.464 for TM3. Similarly, the principle components of PC2 and PC3 of 1984 are composed of opposite factor loadings. Negative Eigen values were observed in all of the main components of the 1990 which affects visual interpretation of the image. Reflection values in the first three principal component images are associated with water surfaces, dune areas and vegetation areas. According to Figure 5, light blue (cyan) color corresponds to irrigated fields, dunes and bare areas represented in pink tones and, dark blue and green tones indicate water surface.

The principle component transformation results for the 2000 are similar to the first three component factor loads of 1984, 2010 and 2011. However, among these components, TM1 load factor has been negative. This allows PC1 to become important for water surface reflection. Water surfaces are shown in shades of pink on the PC image of 2000. In the main component conversions, the remaining data content from the fourth component (including PC5 and PC6) is only about 0.5% of the total. Thus, it is difficult to interpret and monitor land cover changes due to significant noise impact on the resultant images of these components.

TM4, TM2 and TM3 PCA

Beside reflection properties of the water surfaces, wetland and sand dune plants along with different agricultural plant species, which are mainly rice, corn and wheat, are effective in image statistics of the data set used in this study. The main purpose of the PCA and image processing is to bring together the different information and to highlight the required knowledge. According to correlations among bands which are shown in Table 4.10, TM2, TM3 and TM4 are highly correlated with each other. When the results of PCA applied separately to the images from each year were examined, it can be seen clearly that the factor loadings of Landsat TM2, TM3 and TM4 bands gained both negative and positive high values, especially for PC1. Therefore, PCA was reapplied again on TM2, TM3 and TM4 bands as separate data set for each year (Figure 6).

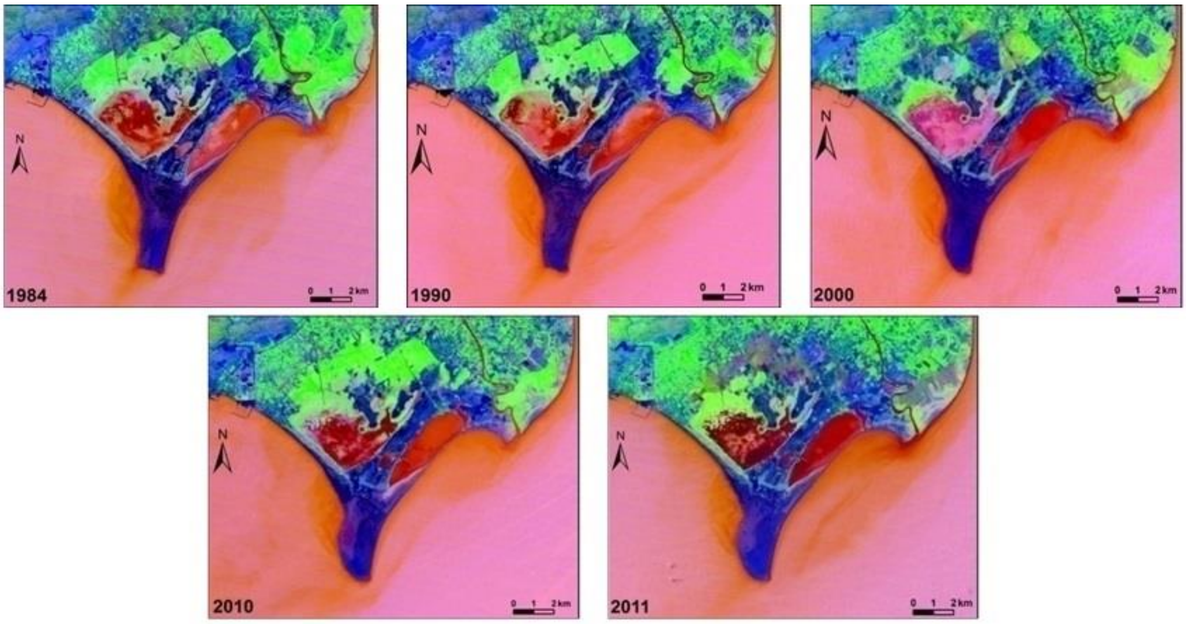

Figure 6: Analysis of Main Components of Landsat TM4, TM3 and TM2 Bands (RGB: PC1PC2PC3)

Unlike the PCA for all bands, the transformations were obtained on the same scale in the PCA of the TM4, TM2 and TM3 bands produced for all years. The factor loadings and the Eigen values of the components are given in Table 4. The low moisture content dunes and the uncovered areas are considered as negative load factor on PC1 which is produced from summer season images. In PC2 component, a maximum positive factor load is calculated for TM4. On the other hand, in PC3 component maximum positive load factor is obtained for the TM3 band. According to results, green areas in Figure 6 indicate regions where the vegetation reflection is abundant and dark blue tone represents regions where the plant signal is not taken. Deep sea areas with low sediment and organic matter content are seen in shades of pink and the lake areas with high sediment content depicted in a dark red color. Sediment transport areas associated with sea currents in coastal areas can be traced with light to dark pink color. Sediment and organic matter content of Akgöl appears to be lower during the years of 1990 and 2000 than in other years. Wetland plants around Akgöl cover less area in the years of 1984 and 1990; however, those areas have increased over the years. On the contrary, although wetland plants are abundant in the eastern part of the Göksu river mouth during the early time of the study period, it is observed that the density of plants decreased in the following years.

Table 4: Analysis of Main Components of Landsat TM4, TM3 and TM2 Bands, Eigen Values and Factor Loads Results

1984

Eigenvectors	PC 1	PC 2	PC 3
TM 2	-0.291	-0.443	-0.848
TM 3	-0.508	-0.679	0.529
TM 4	-0.810	0.585	-0.028
Eigenvalues	2032.72	262.13	8.292
Information%	88.258	11.3813	0.360

1990

Eigenvectors	PC 1	PC 2	PC 3
TM 2	-0.309	-0.484	-0.818
TM 3	-0.470	-0.669	0.574
TM 4	-0.826	0.563	-0.021
Eigenvalues	1556.7	190.665	6.741
Information %	88.75	10.869	0.384

2000

Eigenvectors	PC 1	PC 2	PC 3
TM 2	-0.304	-0.535	-0.787
TM 3	-0.478	-0.629	0.613
TM 4	-0.824	0.562	-0.064
Eigenvalues	1384.22	88.18	5.00
Information %	93.69	5.96	0.34

2010

Eigenvectors	PC 1	PC 2	PC 3
TM 2	-0.304	-0.510	-0.804
TM 3	-0.497	-0.636	0.591
TM 4	-0.8137	0.579	-0.060
Eigenvalues	1488.937	214.64	8.24
Information%	86.98	12.54	0.48

2011

Eigenvectors	PC 1	PC 2	PC 3
TM 2	-0.302	-0.525	-0.795
TM 3	-0.516	-0.610	0.6005
TM 4	-0.801	0.592	-0.087
Eigenvalues	1164.10	138.0	6.109
Information %	88.98	10.54	0.46

TM 5, TM4 and TM1 PCA

According to combined image (TM5, TM4 and TM1), some land cover features, such as wet surfaces and plant areas, which are not distinguished by visible region reflections, are better separated in the infrared wavelength region (Figure 7). At the same time, the lowest correlations were found in the image data sets of TM1, TM4 and TM5 bands. The relationship between near infrared and blue wavelength is low because they are located in different regions of the electromagnetic spectrum. The results also show that variation of the information content of each band is high. Bare land, vegetation, water surface and moist areas can be visually separated on the Landsat TM1, TM4 and TM5 band combination image in the study area. In order to test separability of land cover types around wetlands, PCA has performed on selected bands (TM1, TM4 and TM5) for each year separately (Figure 7). Similar to the PCA results of all bands, different factor loads were calculated for these bands (Table 5). This conversion which took place on a different scale represents that climate variability (such as high precipitation) in years of image acquisition affects the reflection properties obtained from the field. For example, it is possible to see this situation on images of 1990 (dry) and 2011 (wet). These visually indistinguishable differences in raw satellite images can be clearly detected via PCA.

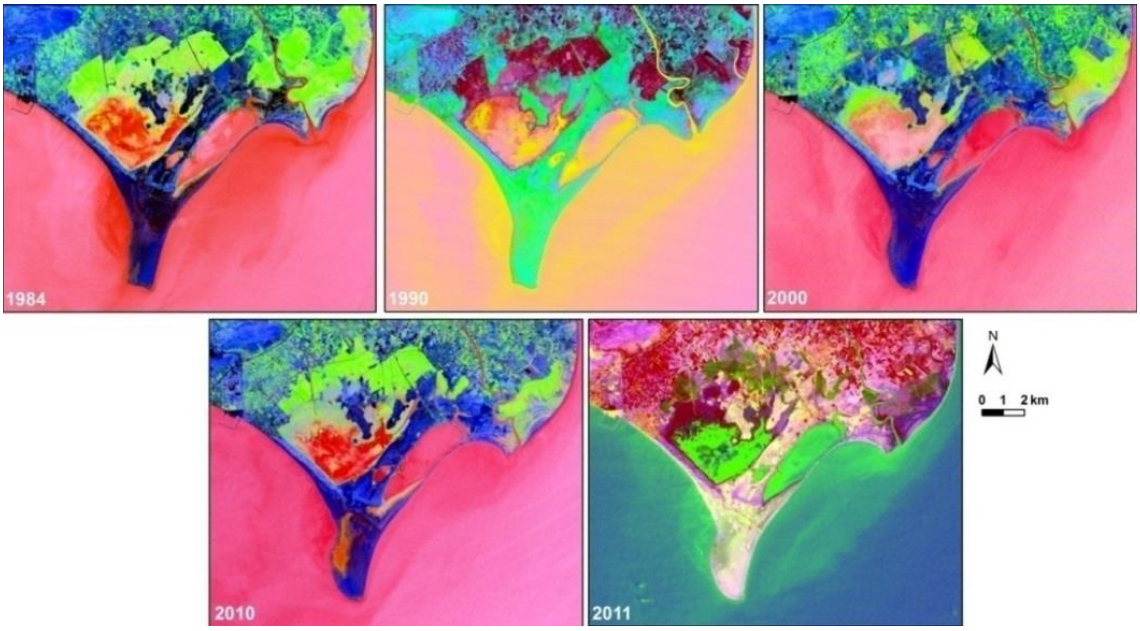

Figure 7: Analysis of the main components of the TM1, TM4 and TM5 band combination (RGB: PC1, PC2, PC3).

Table 5: Analysis of Main Components of TM1, TM4 and TM5 Band Combination Eigen Values and Factor Loads

03 August 1984

Eigen Vectors	PC 1	PC 2	PC 3
TM 1	-0,18383	-0,55048	-0,81436
TM 4	-0,70911	0,64800	-0,27796
TM 5	-0,68072	-0,52637	0,50947
Eigen values	4442,61	373,983	116,39
%	90,059	7,581	2,359

04 August 1990

Eigen vectors	PC 1	PC 2	PC 3
TM 1	-0,16499	-0,50489	-0,84727
TM 4	0,66638	-0,69038	0,28163
TM 5	-0,72713	-0,51814	0,45035
Eigen values	3789,13	254,598	75,649
%	91,98	6,18	1,83

30 July 2000

Eigen vectors	PC 1	PC 2	PC 3
TM 1	-0,15052	-0,49188	-0,85755
TM 4	-0,87604	0,46836	-0,11488
TM 5	-0,45815	-0,73396	0,5014
Eigen values	3494,18	120,757	43,787
%	95,5	3,3	1,19

27 August 2010

Eigen vectors	PC 1	PC 2	PC 3
TM 1	-0,13859	-0,51626	-0,84514
TM 4	-0,82902	0,52732	-0,18617
TM 5	-0,54178	-0,67484	0,50107
Eigen values	3492,48	253,137	84,61
%	84,82	2,93	1,06

13 July 2011

Eigen Vectors	PC 1	PC 2	PC 3
TM 1	0,11264	0,47893	0,8706
TM 4	0,96172	-0,27282	0,02565
TM 5	-0,2498	-0,83439	0,49133
Eigen values	3173,14	157,697	72,832
%	93,22	4,63	2,13

PC1 factor loadings in all components are calculated to be negative for the years of 1984, 2000 and 2010. As can be seen in Figure 7, the PC1 represents mainly water surface reflections, while PC2 depicts vegetation and final principle component shows reflections of dry soil and Dune areas. On the images of these years, light pink tone corresponds water where the surface currents and turbulence are minimal. On the other hand, dark pink tone can be termed as highly turbulent water with abundant sediment and organic matter content. Areas with high humidity in coastal and upland areas are shown with dark orange and light brown tone. In particular, the paddy fields are inseparable from wetland plants clearly due to their similar color tone appearance. In the 1990 PCA transformation, TM4 band has a high factor load on the PC2 (0,69) and PC3 (0,28) components. At the same time, PC of TM4 for the year of 1990, unlike other years, produces the opposite sign in the factor loadings. In the case of TM5, TM4 and TM1 in-band analysis reveals that the plant reflection properties intensified on PC2 as well as on PC1. On the PC of the 1990 image, vegetation in maroon, sand dune areas in green and water is found in yellow and pink tone. TM1 has positive load in 2011. However, the TM4 component has the highest (0.96) and the lowest (0.02) positive factor loads on the PC1 and PC3 in the entire data set. Likewise, for PC3 of 2011, unlike other years, all factor loads were positive. On the PC image of 2011, PC1 can be termed as vegetation due to high NIR reflection (shades of red), PC2 could be representing wetlands (Green) and PC3 depicts water surface with less sediment concentration (blue) (Figure 7).

It should be noted that the PCA for all years calculated on different scales in different years complicates the interpretation of all years in a similar way. Therefore, it is better to create the analysis for each year separately for more accurate assessments.

Change Detection with PCA

In the change detection analysis, the PCA technique could be used in two different ways. In the first method, images for each year are converted into PC's. Thus, the changes that occurred in the study area can be monitored by using principle component analysis images or classified products from PC results. However, in this method, it is not possible to perform "from to" analysis for change detection of land cover/use. In the second method, PCs are produced by combining images from different years (The second method involves combining images from different years and applying them to the analysis of the PCs). Thus, the changes can be assessed by relating the wave length and the associated factor loads in the main components.

According to the results that red and near infrared wavelengths used in the calculation of vegetation indices are also useful in principle component analysis to detect changes in the study area. At the same time, in coastal areas, the change of sediment concentration which is caused by sea currents can be monitored using PCA.

PCs calculated from entire data sets and TM1, TM4 and TM5 bands gave results in different scales. Therefore, analysis was not conducted with the combination of other wavelengths outside the bands of TM2, TM3 and TM4, because of scale differences of transformations.

Three bands (TM2, TM3 and TM4, green, red and near infrared respectively) from all years were combined into 12-band image for change detection via PC (Table 6). According to results that PC1 contains 85.55% of the total variance on the combined image of all years. For PC1, high factor loads in the near infrared region were observed in years of 1984 (-0,293), 1990 (-0,334) and 2010 (-0,538). The 2011 TM3 gives the highest positive load (0.27) in the first component). On the PC2, the green wavelength of 2011 has the highest positive loading (0.251), while the year 1984 has the highest negative loading (-0,508). It is clear from the results that vegetation activities and sand dunes have a significant effect on PC1 of 12-band combined image (Figure 8). At the same time, PC1 could also be representing dry soil and man-made structures on the Göksu delta. In Figure 8, pinkish red hues indicate less changed sand dunes and residential areas.

Table 6: Analysis of the Main Components of TM2, TM3 and TM4 Composition Eigen Values and Factor Loads

		PC 1	PC 2	PC 3	PC 4	PC 5	PC 6	PC 7	PC 8	PC 9	PC 10	PC 11	PC 12	PC 13	PC 14	PC 15
1984	2	0.151	0.228	0.436	0.141	0.220	0.369	0.130	0.227	0.337	0.129	0.219	0.359	0.112	0.199	0.31
	3	-0.287	-0.354	0.332	-0.214	-0.268	0.320	-0.136	-0.158	0.200	-0.281	-0.347	0.236	-0.210	-0.248	0.11
	4	-0.293	-0.508	-0.302	-0.125	-0.272	0.016	0.067	0.066	0.006	0.238	0.271	0.230	0.299	0.406	0.15
1990	2	0.075	0.248	-0.080	-0.229	-0.206	-0.215	-0.293	-0.353	0.040	0.191	0.439	0.139	-0.256	-0.255	0.43
	3	0.096	0.008	0.645	-0.122	-0.292	0.001	-0.119	-0.280	-0.339	0.157	0.105	-0.260	0.243	0.270	-0.17
	4	-0.334	-0.405	0.176	0.304	0.540	0.063	-0.128	-0.152	-0.087	0.163	0.321	-0.255	-0.157	-0.185	0.05
2000	2	0.075	0.075	-0.189	0.215	0.291	0.117	-0.309	-0.524	-0.271	-0.142	-0.245	0.420	0.171	0.272	0.04
	3	-0.114	-0.084	0.311	-0.010	0.125	-0.665	0.035	0.155	-0.067	-0.012	0.029	0.556	-0.101	-0.025	-0.26
	4	-0.009	0.103	-0.136	-0.100	-0.074	0.482	-0.049	0.029	-0.160	0.185	0.319	0.293	-0.192	-0.171	-0.63
2010	2	-0.363	0.253	-0.006	-0.359	0.197	0.007	-0.320	0.170	0.073	-0.414	0.193	-0.158	-0.198	0.470	-0.06
	3	0.048	-0.034	-0.033	0.061	0.006	-0.146	-0.136	-0.369	0.781	0.122	0.011	-0.097	0.133	0.097	-0.39
	4	-0.538	0.373	0.002	-0.290	0.185	0.010	0.093	-0.053	-0.016	0.484	-0.337	-0.001	0.257	-0.153	0.03
2011	2	-0.375	0.251	0.011	0.273	-0.189	-0.012	0.590	-0.361	-0.011	-0.369	0.258	0.022	0.030	-0.014	-0.01
	3	0.269	-0.184	-0.008	-0.492	0.317	0.024	0.514	-0.303	-0.015	0.102	-0.068	-0.011	-0.354	0.226	0.01
	4	-0.153	0.108	0.002	0.407	-0.262	-0.011	-0.018	0.021	0.001	0.367	-0.254	-0.027	-0.613	0.388	0.02
EV		7370	648.8	146.4	93.94	82.95	73.91	59.46	45.04	42.26	22.6	20.9	3.21	1.95	1.56	1.34
%		85.55	7.53	1.69	1.09	0.96	0.85	0.69	0.52	0.49	0.26	0.243	0.037	0.022	0.018	0.015

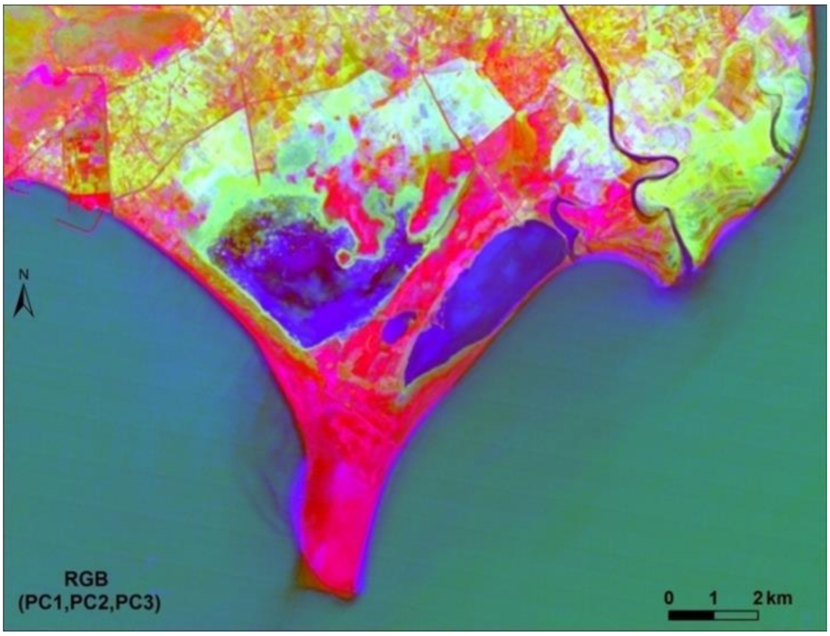

Figure 8: Combined Image Data Set Main Components Analysis Result Image

In PC2 component, reflection characteristics associated with plant activity can be seen in green-yellow color tones. At the same time, PC2 also contains information mainly from 1984 image. The changes that have occurred in the area of water and dunes are seen in the violet-blue tones for the PC3. High Eigen values reveal effect of low sediment and organic matter content of water areas along with vegetation activities (due to high reflections in TM4) on the composite image.

Because factor loadings for all data sets show similar distribution characteristics, areas of change could not be clearly identified on the PC1 image. RGB combination image is created by using first, second and third principle component data with variance of around 10% (Figure 9). Unlike the color combination of first three principle components, the color composite of second, third and fourth Eigen images depicts changed as well as unchanged areas, clearly. Increase of dry land, dune and residential areas are represented in shades of light blue. Decreases of these areas are also depicted in dark purple and maroon color tones. Notice the light green coloring on water surfaces of Akgöl, Paradeniz lakes and Göksu river, indicating changes of sediment concentration with increasing trend. Changes associated with vegetation cover differed depending on the land use and cover types. Changed and unchanged wetland areas around lakes (especially Akgöl) are shown in different color such as white tone representing unchanged regions and purple tone indicating increasing vegetation areas. Variations related to the cropping cycle in irrigated paddy fields (within different data acquisition dates) are seen in the yellow tone.

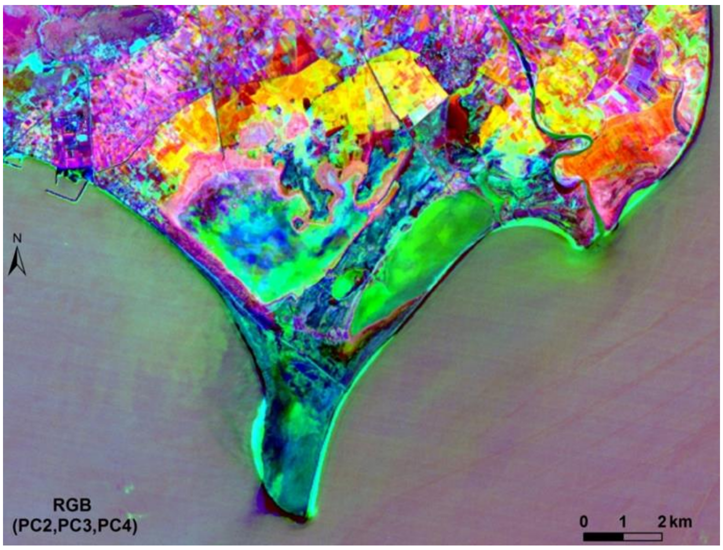

Figure 9: Combined Image PC2, PC3 and PC4 Combination of Main Components

Beside wavelength range, the year of image that becomes prominent in the data set have a significant effect on factor loadings during the change detection analysis using images from different dates. From the loadings for PC1, we see that this component is strongly correlated with the image years of 2010 and 2011. On the other hand, loadings for PC2 represent high correlation in 1984 and 2010 image data sets. For detailed analysis in the first stage, density distribution graph was created using PC2 and PC3 (Figure 10). Due to the water surface covering a large area in the study area (approximately 50%), significant amount of data (red and green) which belong to the sea accumulated in the region near zero on the chart. While negative PC2 and positive PC3 densities refer to wetlands areas, increased intensity of the light blue area shows the reflection values of vegetation in PC2. Likewise, the other light blue tone on PC2 and PC3 located in the cluster area of the negative zone indicates bare dune fields, wet dunes and sparse dune plants. The relatively low density values shown on the graph (purple) refer to changes that occur in different spatial context.

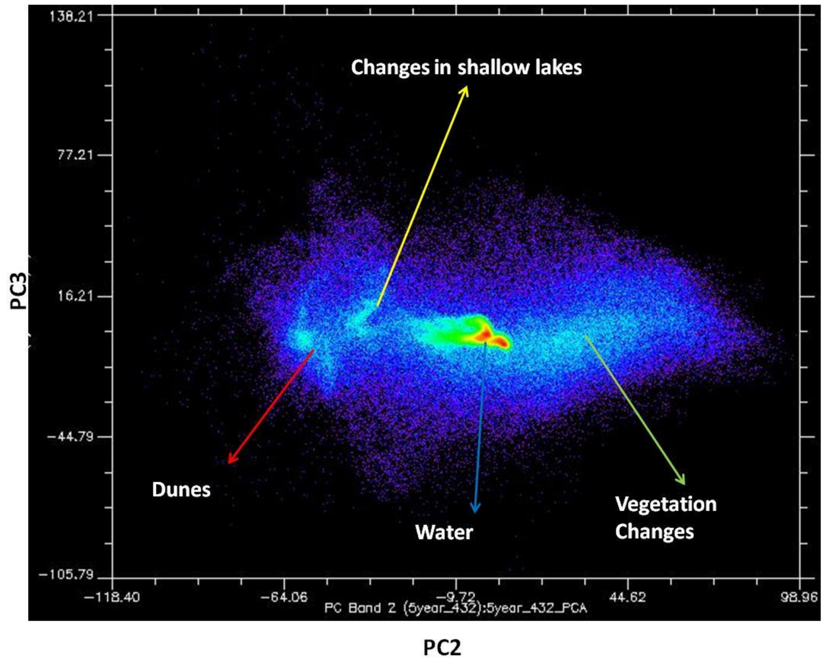

Figure 10: Scatter Graphic of PC2 and PC3

The PC1 image is matched with the data distribution graph of new components calculated from the combined images for all years (Figure 11). The negative values which are shown with yellow color in the image of PC2 and PC3 indicate the change in the direction of reduction. This data region indicates the decline in vegetation and wet surfaces on the dune as well as the decline in dune areas. In the interior section of the study area decreasing trend is emerging in some agricultural and residential areas. The red color (PC3 positive, PC2 negative values) is assigned for the incremental land cover. These regions would be associated with an increasing rate of sand dunes and sediment contents of lakes. Light green colors are observed especially in areas where the paddy cultivation extensive. In these fields where each of the components (PC2 and PC3) has a positive value, changes are more related to plant activity than areal differentiation. It relates to a new start of plant activity on paddy fields during the image acquisition date of July 13’th of 2011.The Regions with purple tones on PC2 (positive) and PC3 (negative) are labeled as changing areas toward a reduction in plant activity. The rate of change in wetland plants could not be distinguished by the method of clustering on the graph of these two components. It is found that reflections of agricultural fields and wetland plants located to the east of the Göksu River are especially undistinguishable from each other. It is concluded that PC2 and PC3 components cannot therefore be used to detect changes associated with wetland plants in the Göksu delta.

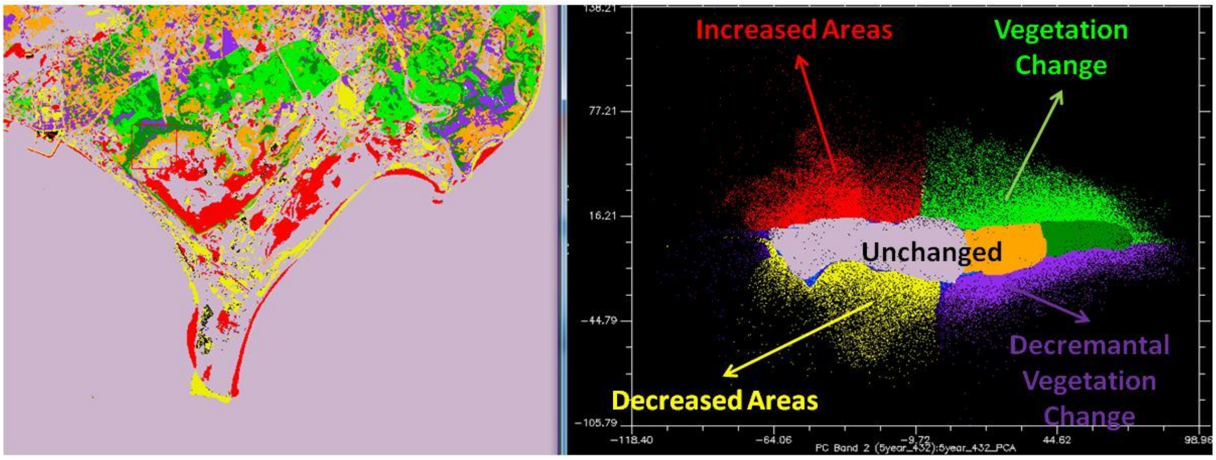

Figure 11: Change Classes According to PC2 and PC3 of Principal Component Data Set

The scatter diagram for PC3 and PC4 has been created to interpret the blue, green and red component image, visually. Land cover classes and changed areas have been matched with PC3 by using a scatter diagram above mentioned (Figure 12). It is clear that the tendency of clustering tends to decrease in PC3 and PC4 as Compared to PC2 and PC3 graph. This condition is associated with data content reduction and an increased level of noise, till the next component. While increased dune areas and lake sediment (blue) have high positive loadings on PC3 and PC4, declining dune areas and agricultural fields correspond to negative values in both components. Changes arising from the relationship between image acquisition dates and paddy farming activities are represented in green color. Due to the aggregation of data on graphic origin and nearby regions, discrimination of changes has become difficult and thus, these areas appointed as unchanged fields on the graph (Figure 12).

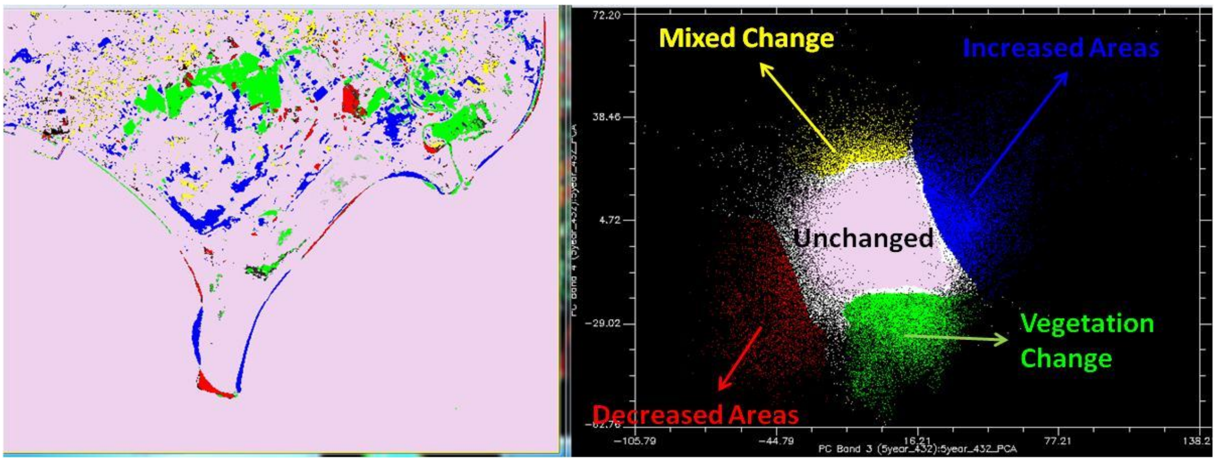

Figure 12: Change Classes According to PC3 and PC4 of Principal Component Data Set

In order to elaborate changes that occurred in wetland areas, despite of the low data variance, PC4, PC5, and PC6 components (RGB) image was created due to the relatively high factor loadings (Figure 13). While all factor loadings are positive on PC6 for the year of 1984, quite high factor loadings in 2011 were calculated, similarly. PC5 for the 1990 image has the highest factor loading of 0.540 from TM4 (near infrared). The distribution of wetland plants can be seen more clearly in the image that produced via a combination of these components. Especially, increased wetland plants around Akgöl can be traced in red tones (Figure 13).

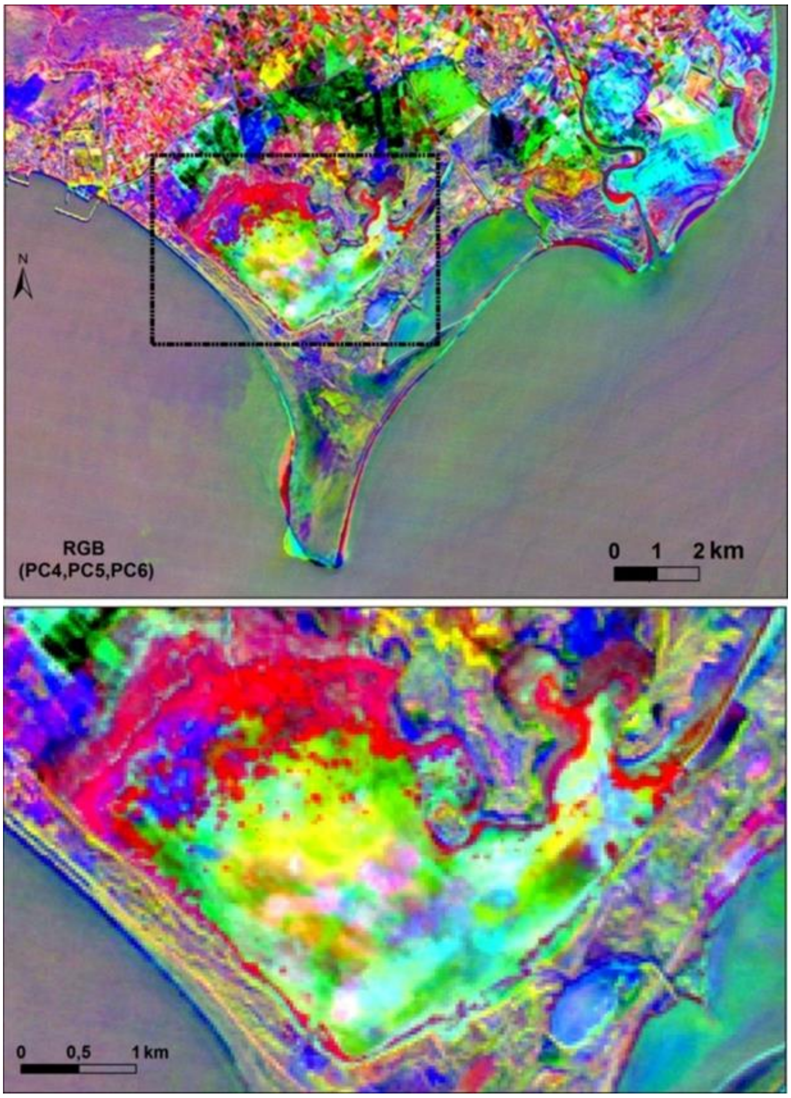

Figure 13: Combined Image PC4, PC5 and PC6 Combination of Main Components and Distribution of Wetland Plants Around Akgöl

Classification of the results of the combined PCA

In remote sensing, one of the commonly used image processing techniques to determine the type of land cover/use is a classification method. Depending on the characteristics of the image data and method; remotely sensed data are used in various studies such as monitoring of urban development, watershed management, natural disasters and risk analysis. However, classification analysis is difficult in areas where the reflection properties of the land vary over short distances such as mixed plant environments and wetlands. Therefore, in remote sensing studies, land cover heterogeneity arises as a limiting factor along with spatial and spectral resolution characteristics. Surface reflection properties are confused with each other where the dense wetland plants and agricultural activities are located closely. As stated in the work of Özesmi and Bauer (2002), due to the interference of the reflection properties of wetland plants (such as Juncus and Phragmites), their separation is not an easy task to complete during the direct classification procedures. In contrast, surface water with low sediment and organic matter content can be easily distinguished.

In order to measure the areal changes of land cover in the Göksu delta, PCA results produced from the merged images of TM2, TM3 and TM4 are classified with unsupervised classification technique. Before classification procedures, separability of classes on the data distribution chart was examined for the PC1 and the PC2 (Figure 14). Results showed that the changes cannot be clearly separated on the first principle component during visual interpretation. However, it is clear that the distribution of land use clusters became apparent on the scatter graph. As in the near infrared and red wavelengths scatter chart, reflection values of water surfaces have concentrated on negative side of scatter plot of PC1 and PC2. According to results, terrestrial plant reflection values clustered at the positive side of PC2 and wetland plants located on the negative region of PC1 and reflections of agricultural land gathered on the positive side of PC1.

Reflections of sand dunes, dune plants and bare land have aggregated on both the positive and negative regions of PC1 and PC2 (Figure 14).

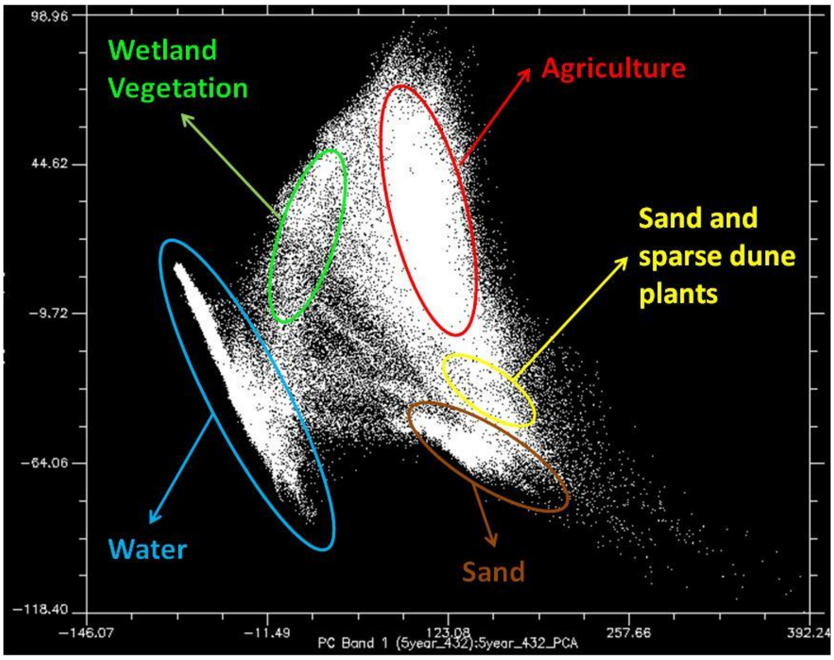

Figure 14: Land Cover Classes on PC1 and PC2 Scatter Plots

In the first stage, first and second principle component bands are classified together (Figure 15). Although reflection properties of agricultural areas (light green tone) mixed with some dune plants on the scatter diagram, these land cover classes were included in a separate class in the resultant image. In the study area, changes associated with coastal progress and marine regression, dune moisture content and Göksu river bed changes are assigned to one class labeled as sand dune changes (red). However, the increase or decrease in the direction of coastal changes occurring is inseparable with the classification of PC1 and PC2. Although mixed land cover classes show changes in dune areas and residential areas; this class also includes harvested or unplanted agricultural areas and newly established residential fields.

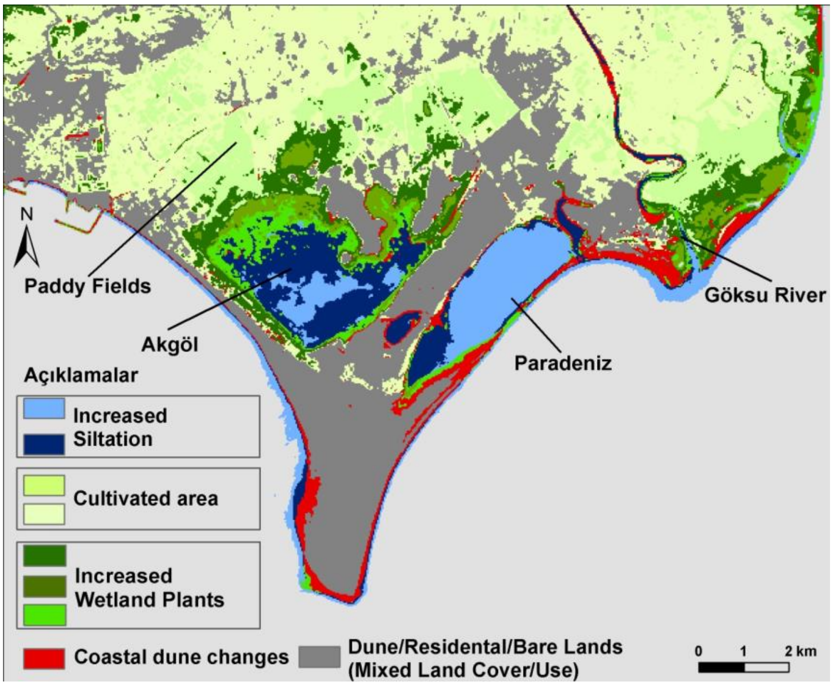

Figure 15: Unsupervised Classification Result of PC1 and PC2 Layers Stack

Changes on the water surface and wetlands areas around Akgöl can be easily detected on the classification image of the first two principal components. Wetland plants in the image of 1984 are shown in dark green tone. This class also represents similar reflections with paddy cultivation areas. On the other hand, the wetland plants (assigned to the olive green tone), which increased after 1984, are seen both around Akgöl and east of the Göksu river. Especially in the area of approximately 30 hectares burned in 2000 in the north of Akgöl, however wetland plants have redeveloped in the following years. It is noted that wetland plants showed a significant increase during the period of 1984-2011 (assigned to light green) in south of Paradeniz and in the interior parts of the Akgöl. Developing wetland plants during the 27 year-time period cover an area of approximately 188 hectares in Akgöl. Dark blue labeled sections indicate areas where the sediment and organic matter content increased which are parallel with the direction of wetland plant developments Areas in the Akgöl and Swan lakes, labeled as dark blue, are regions of increased sediment and organic matter content. The areas of increase in sediment and organic matter content are parallel to the development direction of wetland plants in Akgöl.

The first six components that have the image data variance of 97.67% PCA were classified using unsupervised classification technique in order to determine changes in more detail (Figure 16). Total 15 classes were specified on the resultant image that four of these classes represent water surfaces and wetland plants were likewise grouped into four classes. Unlike classification results of PC1 and PC2 combination, increase and decrease occurring in the coastal dunes is clustered in separate classes in the six-band principle component classification image. However, the changes in the moisture content in sand dune areas, the changes that occur in urban areas, bare land and some agricultural areas are not clearly separable. Therefore, these classes have been tagged in mixed land cover classes. Although sand dunes, residential areas and bare lands can be distinguished from each other on PC1 and PC2 image, distinctions within the class cannot be made (Dunes, settlements and uncovered areas are visually more pronounced in the classification results of PC1 and PC2, but no distinction can be made within the class).

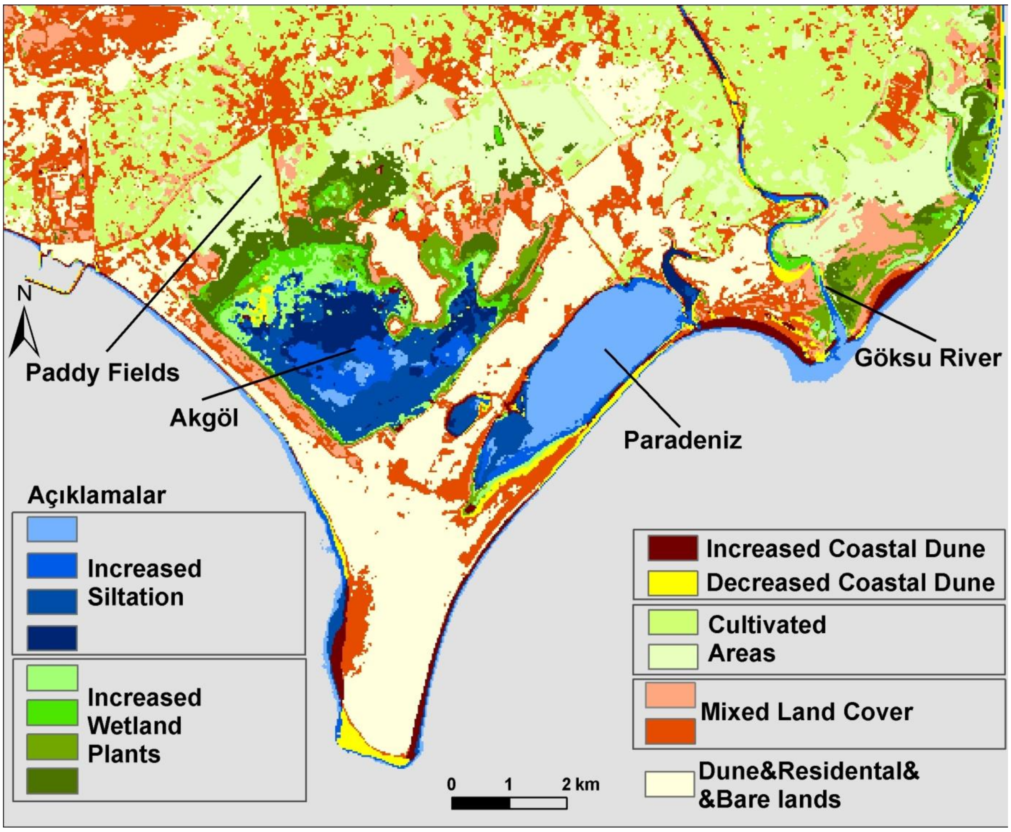

Figure 16: Unsupervised Classification Result of the First Six of Principal Components (From PC1 to PC6)

Four classes were identified to express changes that occurred on the lake water surface for the period of 1984 and 2011. The lake Paradeniz has preserved the overall condition in the study period, except increasing sediment content in the south side of lake. Akgöl water surface area shows the trend of decline depending on the areal expansion of aquatic plant which is associated with an upward tendency of the sediment and organic matter content (Figure 17). Burning area in 2000 (in black circles) which is located in the north of Akgöl leads to the emergence of changes in more detail between years. The burned area has been measured around 30 hectares in the first classification, on the other hand 24 hectares found in the second classification. Distribution area of wetland plants around the entire lake was about 345 hectares in 1984 and showed an increase in the total of 197 hectares in following years. Development trends in wetland plants indicate a disadvantageous situation against Akgol in the northwest part of the lake (Figure 17).

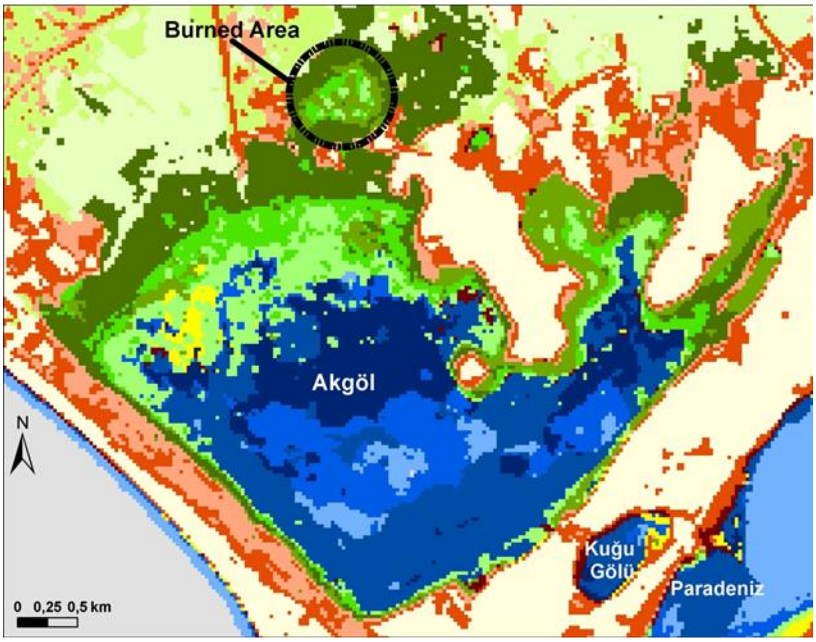

Figure 17: Closer View of Unsupervised Classification Result of the First Six of Principal Components (From PC1 to PC6)

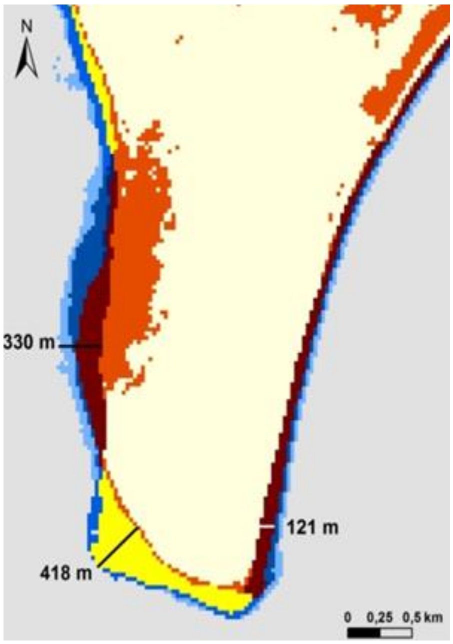

Figure 18: İncekum Cape Coastal Progression (Brown) and Coastal Regression (Yellow) Areas

Dune progression and regression activities caused a significant amount of shoreline changes in İncekum foreland during the study period (Figure 18). It is concluded that approximately 330 m the shoreline advances measured on the İncekum foreland. Along with this progress, the area of 54 hectares of sand dune has been added to the shore (Brown-Dark blue). Similarly along the east of İncekum cape, total of 33 hectares of expansion have occurred along with 121 meters shoreline advances. To the south of the cape, about 29,7 hectares of dune area (yellow color) was eroded due to coastal erosion in the length of 448 m. Despite the shortening of the size of the İncekum cape, it has expanded significantly during the 27 years. On the İncekum, mixed land class represented by the orange label that specifying the increase in the moisture content of the western region and it represents the change in dune vegetation on the northeastern part of the area.

The changes in the region of the mouth of the Göksu River are quite dynamic due to sea currents that flow in and around the river mouth. The shoreline which is located on the southeast side of the Göksu River mouth is dominated by the coastal progression (Figure 19). During the study period, marine depositional areas are developed reaching a maximum width 230 m to the east and 173 m west of the river mouth. These depositional areas cover 18.8 hectares in the East and 34.9 hectares in the West. Similarly, at the north of the mouth of the Goksu River, 245 m changes are also measured. River flood areas (labeled in light green and yellow tones) are indistinguishable because of mixing of the sand dune and vegetation increase classes. While change is not observed in the lake area of Paradeniz except for the southern part of the lake, in dune areas forming the boundary with the sea, it is measured that approximately 110 m regressions have occurred (Figure 19). According to the principle component classification results, it found that agriculture, wetland, sand dune plants and residential areas cannot be clearly separated. Due to complicated reflection properties of the study area, it is difficult to establish 'from-to' analysis using PCA.

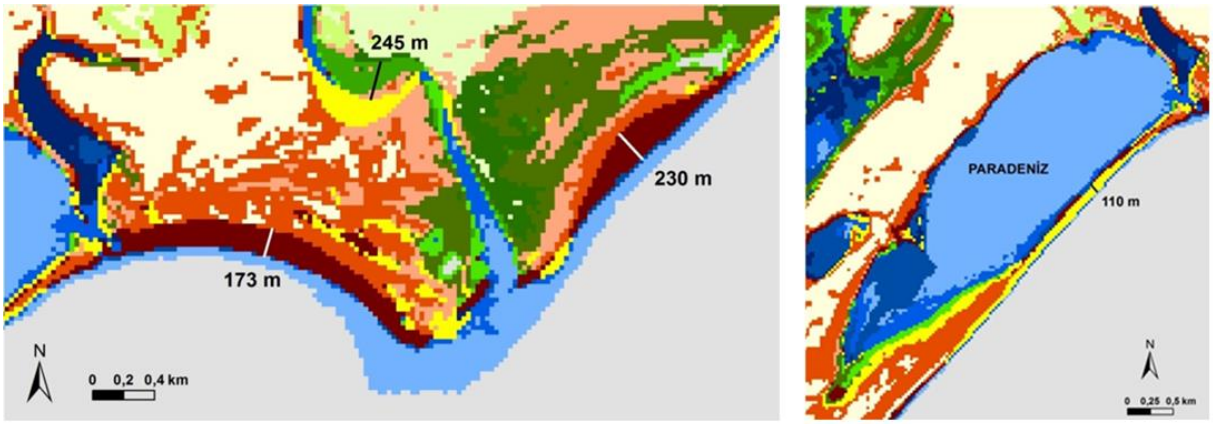

Figure 19: Changes in the Mouth of the Göksu Riverbed and the Lake Paradeniz

CONCLUSION

River deltas with high short and long term surface dynamics are difficult to determine by conventional classification and change detection methods using remotely sensed data due to the complex and dynamic land cover/use characteristics. These complex areas are constantly having dynamic change systems demonstrating distinctive land processes and human activities, yet identifying them may be difficult because of the large number of confusing pixels and the ambiguity on land cover transformations. In this study, the major land cover/use and coastal change patterns and trends of the Göksu delta were examined by using the principal component transformation of a dataset of Landsat TM covering four different dates. We used PCA because it has proved to be an excellent pixel based change detection technique in many studies. Using a PCA method, this study is able to determine major changes of Göksu delta wetlands and coastal zones which represent spatially and temporally heterogeneous character.

It has been tested that TM2, TM3 and TM4 were the appropriate bands for PCA. Therefore, determining the transitions of land cover and coastal changes was facilitated by using TM2, TM3 and TM4 into PCA transformations to extract joint patterns of variation among complementary multi-spectral Landsat data. The primary benefit of using those bands was in highlighting prevalent condition of landscape that constituted large components of the area, even for classes with smaller spatial extent. In addition, final PCA revealed the dominant temporal pathways of wetland and coastal change. This technique effectively highlighted major locations and directions of change in the area and was able to find key differences among the years. Changing the water content and quality of wetlands were identified by principal component analysis during the period of the image data set was taken between 1984 and 2011. Beside determination of changes that occurred in and around wetlands, the rate of coastal advancement and regressions has also been calculated effectively. Principal components analysis technique obtained from different band combinations of TM data has produced useful results in this study while mapping and monitoring changes in the Göksu Delta wetlands.

In addition to natural factors, human interventions in the Göksu delta have also been effective in coastal changes. It seems that the reduction of the amount of sediment reaching the delta by the Gezende dam, which was operated in 1992, has significantly affected the development of the delta. There are 8 dam projects planned to be built on the Göksu River along with Kayraktepe Dam (Karaömerlioğlu, 2007). It is thought that these dams planned to be constructed will affect the development of delta in the negative direction because the erosion, transport and accumulation activities of the rivers carrying material to the delta will be weakened and the delta development will be affected negatively. Although the delta area is protected by many legal statuses, any changes in the Göksu river basin affect the delta directly. Therefore, when preparing management and conservation plans, the whole basin should be taken into account and planning should be done in this framework.

Acknowledgments

This study is supported financially by The Scientific and Technological Research Council of Turkey (TUBİTAK ÇAYDAG project No. 110Y295)

Kaynakça / References

Adam, E., Mutanga, O. & Rugege, D. (2010). Multispectral and hyperspectral remote sensing for identification and mapping of wetland vegetation: a review. *Wetlands Ecology and Management,* 18, 281–296.

Almutairi, A. & Warner, T. A. (2010). Change detection accuracy and image properties: a study using simulated data. *Remote Sensing*, 2(6), 1508-1529.

Artigas, F. J. & Yang, J. (2006). Spectral discrimination of marsh vegetation types in The New Jersey Meadowlands, USA. *Wetlands Journal of the Society of Wetland Scientists,* 26, 271–277.

Balázs, B., Bíró, T., Dyke, G., Singh, S. K. & Szabó, S. (2018). Extracting water-related features using reflectance data and principal component analysis of Landsat images. *Hydrological Sciences Journal*, 63(2), 269-284.

De Roeck, E. R., Verhoest, N. E., Miya, M. H., Lievens, H., Batelaan, O., Thomas, A. & Brendonck, L. (2008). Remote sensing and wetland ecology: a South African Case Study. *Sensors,* 8, 3542-3556.

Deng, J. S., Wang, K., Deng, Y. H. & Qi, G. J. (2008). PCA-based land-use change detection and analysis using multitemporal and multisensor satellite data. *International Journal of Remote Sensing*, 29(16), 4823–4838.

Ghioca-Robrecht, D. M., Johnston, C. A. & Tulbure, M. G. (2008). Assessing the use of multiseason QuickBird imagery for mapping invasive species in a Lake Erie coastal Marsh. *Wetlands* 28, 1028–1039.

Gilmore, M. S., Wilson, E. H, Barrett, N., Civco, D. L., Prisloe, S., Hurd, J. D. & Chadwick, C. (2008). Integrating multi-temporal spectral and structural information to map wetland vegetation in a lower Connecticut River tidal marsh. *Remote Sensing of Environment* 112, 4048–4060.

Gürkan, F., Zorlu, F., Kavruk, S.A., Menengiç, M., Yıldırım, N., Erdogan, B., Direk, Y., Buluş, B. & Sarıgül, B. (1999). *Göksu Deltası özel çevre koruma bölgesi yönetim planı*. Çevre Bakanlığı ÖÇKK Başkanlığı-DHKD, Ankara-Turkey.

Hardisky, M. A, Gross, M. F. & Klemas, V. (1986). Remote sensing of coastal wetlands. *Bioscience,* 36, 453–460.

Hinrichsen, D. (1998). *Coastal Waters of the World: Trends, Threats, and Strategies*, USA. Washington, DC: Island Press.

Jensen, J. R. (1996). *Introductory Digital Image Processing: A Remote Sensing Perspective*. New Jersey: Englewood Cliffs.

Karabulut, M. (2007). Su içerisinde yaşayan bitkilerin spektral özelliklerinin incelenmesi. *İtü Dergisi/D-Mühendislik Serisi,* 6(3), 3-10.

Karabulut, M. (2015). Farklı uzaktan algılama teknikleri kullanılarak göksu deltası göllerinde zamansal değişimlerin incelenmesi. *The Journal of International Social Research* 8(37), 347-363.

Karaömerlioğlu, D. (2007). *Göksu Deltası'ndaki (Silifke) doğal ekosistemlerin bitki ekolojisi yönünden araştırılması.* (Doktora Tezi, Çukurova Üniversitesi, Fen Bilimleri Enstitüsü, Adana).

Kassawmar, N. T., Rao, K. R. M. & Abraha, G. L. (2011). An integrated approach for spatio-temporal variability analysis of wetlands: a case study of Abaya and Chamo lakes, Ethiopia. *Environmental Monitoring and Assessment*, 180(1-4), 313-324.

Li, X. & Yeh, A. G. O. (2010). Principal component analysis of stacked multi-temporal images for the monitoring of rapid urban expansion in the Pearl River Delta. *International Journal of Remote Sensing*, 19(8), 1501-1518.

Liu, J. G. & Mason, P. (2009). *Essential Image Processing and GIS for Remote Sensing*. Hoboken: John Wiley-Blackwell Pres.

Lu, D., Mausel, P., Brondızıo, E. & Moran, E. (2004). Change detection techniques. *International Journal of Remote Sensing*, 25(12), 2365-2407.

Lunetta, R. S. & Balogh, M. E. (1999). Application of Multi-Temporal Landsat 5 TM imagery for wetland identification, *Photogrammetric Engineering and Remote Sensing,* 65, 1303–1310.

Mishra, D., Narumalani, S., Rundquist, D. & Lawson, M. (2006). Benthic habitat mapping in tropical marine environments using Quickbird multispectral data. *Photogrammetric Engineering and Remote Sensing,* 72, 1037–1048.

Mitsch, W. J. & Gosselink, J. G. (2000). *Wetlands. Canada,* : John Wiley & Sons.

Munyati, C. (2004). Use of Principal Component Analysis (PCA) of remote sensing images in wetland change detection on the Kafue Flats, Zambia. *Geocarto International*, 19(3), 11-22.

Ortiz-Rivera, V., Vélez-Reyes, M. & Roysam, B. (2006). Change detection in hyperspectral imagery using temporal principal components. *Algorithms and Technologies for Multispectral Hyperspectral and Ultraspectral Imagery XII*, 6233, 623312.

Özesmi, S. L. & Bauer, M. E. (2002). Satellite remote sensing of wetland. *Wetland Ecology Management,* 10, 381–402.

Rundquist, D. C., Narumalanı, S. & Narayanan, R. M. (2001). A review of wetlands remote sensing and defining new considerations. *Remote Sensing Reviews*, 20, 207–226.

Silva, T. S. F., Costa, M. P. F., Melack, J. M. & Novo, E. M. L. M. (2008). Remote sensing of aquatic vegetation: theory and applications. *Environmental Monitoring and Assessment,* 140, 131-145.

Tsai, F., Lin, E. K. & Yoshino, K., (2007). Spectrally segmented principal component analysis of hyperspectral imagery for mapping invasive plant species. *International Journal of Remote Sensing*, 28(5), 1023-1039.

Ullah, A., Rundquist, D.C. & Derry, D.P. (2000). Characterizing spectral signatures for three selected emergent aquatic macrophytes: a controlled experiment. *Geocarto International,* 15(4), 31-42.

Yana, H. & Ichikawa, M. (2007). *Factor analysis. In: Handbook of Statistics*. Amsterdam: Elsevier.

Yıldırım, N., Toprak, A., Akdağ, L., Karaca, İ., Kazman, E., Çetin, Y. & Direk, Y. (2009). *Göksu Deltası Özel Çevre Koruma Bölgesi II. Dönem Yönetim Planı.* TC Çevre Bakanlığı ÖÇKK Başkanlığı, Ankara-Türkiye.

Zhang, Y., Lu, D., Yang, B., Sun, C. & Sun, M. (2011). Coastal wetland vegetation classification with a Landsat Thematic Mapper Image. *International Journal of Remote Sensing,* 32(2), 545-561.